

1 **Toxicity, transfer and depuration of anatoxin-a (cyanobacterial neurotoxin)**
2 **in medaka fish exposed by single-dose gavage**

3

4 Simon COLAS¹, Charlotte DUVAL¹ and Benjamin MARIE¹

5 ¹UMR 7245 CNRS/MNHN "Molécules de Communications et Adaptations des Micro-organismes, Muséum
6 national d'Histoire naturelle, Paris – France

7

8

9 **Abstract**

10 The proliferations of cyanobacteria are increasingly prevalent in warm and nutrient-enriched
11 waters and occur in many rivers and water bodies due especially to eutrophication. The aim of
12 this work is to study in female medaka fish the toxicity, the transfer and the depuration of the
13 anatoxin-a, a neurotoxin produced by benthic cyanobacterial biofilms. This work will provide
14 answers regarding acute toxicity induced by single gavage by anatoxin-a and to the risks of
15 exposure by ingestion of contaminated fish flesh, considering that data on these aspects remain
16 particularly limited.

17

18 The oral LD₅₀ of a single dose of (±)-anatoxin-a was determined at 11.50 µg.g⁻¹. First of all,
19 lethal dose (100% from 20 µg.g⁻¹) provokes rapid respiratory paralysis (in 1-2 min) of the fish
20 inducing the death by asphyxia. Noticeably, no death nor apparent neurotoxicologic effect
21 occurred during the experimentation period for the 45 fish exposed to a single sub-acute dose
22 of (±)-anatoxin-a corresponding to the no observable adverse effect level (NOAEL = 6.67 µg.g⁻¹).
23 Subsequently, the toxicokinetics of the (±)-anatoxin-a was observed in the guts, the livers
24 and the muscles of female medaka fish for 10 days.

25 In parallel, a protocol for extraction of anatoxin-a has been optimized beforehand by testing
26 3 different solvents on several matrices, the extraction with 75% methanol + 0.1% formic acid
27 appearing to be the most efficient. Anatoxin-a was quantified by high-resolution qTOF mass
28 spectrometry coupled upstream to a UHPLC chromatographic chain. The toxin could not be
29 detected in the liver after 12 h, and in the gut and muscle after 3 days. The mean clearance rates
30 of (±)-anatoxin-a calculated after 12 h are above 58%, 100% and 90% for the guts, the livers
31 and the muscles, respectively. Non-targeted metabolomics investigations performed on the fish
32 liver indicates that the single sub-acute exposure by gavage induces noticeable metabolome
33 dysregulations, including important phospholipid decreases, with an organism recovery period
34 of above 12-24h. Overall, the medaka fish do not appear to accumulate (±)-anatoxin-a and to
35 largely recover after 24h following a single sub-acute oral liquid exposure at the NOAEL.

36

37 **Keywords:** cyanobacteria; neurotoxin; fish; toxicology; gavage; toxicokinetics.

38

39 **Introduction**

40 Worldwide proliferation of cyanobacterial blooms constitutes a serious environmental and
41 economic problem that menaces wildlife and human health. Moreover, many cyanobacteria are
42 able to produce potent hepatotoxins such as microcystin, cylindrospermopsin and nodularin,
43 and/or neurotoxins such as anatoxins-a, homo-anatoxin-a, anatoxin-a(s) and saxitoxin (Sivonen
44 & Jones, 1999). Harmful cyanobacterial blooms in lakes have been described for decades; in
45 rivers, however, first reports of animal deaths from toxic benthic cyanobacteria in many regions
46 occurred only in the last 20 years (Wood et al., 2007). Since toxic benthic cyanobacteria in
47 rivers have been documented in many countries and benthic taxa have been found to produce a
48 large spectrum of those cyanotoxins, though most animal fatalities reported in relation to
49 benthic cyanobacteria were associated with the presence of anatoxin-a (ANTX) and/or
50 homoanatoxin-a (HANTX) (for review Quiblier et al., 2013).

51 Anatoxin-a and homoanatoxin-a are potent neurotoxins produced by some planktonic and
52 benthic strains of the genera *Anabaena*, *Oscillatoria*, *Aphanizomenon* and *Cylindrospermum*
53 (Bouma-Gerson et al., 2018). Indeed, numerous fatal intoxications of animals, by anatoxin-a
54 and homoanatoxin-a, have been reported all over the world (Gugger et al., 2005; Puschner et
55 al., 2010; Wood et al., 2007). These alkaloids bind tightly to the nicotinic acetylcholine
56 receptor, in the sub-nanomolar range, and thus provoke the death of animals almost
57 immediately after ingestion (Wonnacott and Gallagher, 2006). Anatoxin-a, as a competitive
58 agonist of acetylcholine can bind it specific membrane receptors, notably at neuromuscular
59 junctions, affecting signal transmission between neurons and muscles, causing muscle cell
60 overstimulation (Carmichael, 1994; Aráoz et al. 2010). Acute effects in vertebrates include a
61 rapid loss of coordination, a decreased of locomotor activity, a paralysis of the peripheral
62 skeletal and respiratory muscles, causing symptoms such as loss of coordination, twitching,
63 irregular breathing, tremors, altered gait and convulsions before death by acute asphyxia
64 induced by respiratory arrest (Dittmann and Wiegand, 2006).

65

66 It is maybe because anatoxin-a is very unstable and labile in the water (Stevens and Krieger,
67 1991) and because no chronic effects have been described in mammals so far (Fawell et al.,
68 1999), that this toxin has been considered of less environmental concern comparing to other
69 cyanotoxins. Despite the acute neurotoxic effects of anatoxin-a, the consequence of the
70 proliferation of anatoxins-a producing cyanobacterial biofilms on ecosystem health and aquatic
71 organisms remains largely unknown. Despite, toxic benthic cyanobacterial mats have been
72 associated with decreased macro-invertebrate diversity (Aboal et al., 2002), few studies have
73 investigated the genuine toxicological effects of these compounds on aquatic organisms
74 (Carneiro et al., 2015; Osswald et al., 2007b; Anderson et al., 2018). In some experiments
75 performed on fishes, such as carps and goldfish, behavioural defects such as rapid opercular
76 movement, abnormal swimming (Osswald et al., 2007a) and muscle rigidity (Carmichael et al.,
77 1975) were observed. Oberemm et al. (1999) described also the alterations in heart rates in
78 zebrafish embryos after an exposure to anatoxin-a. Thus a scarcity of information regarding its
79 capability of aquatic species to bio-concentrate and bioaccumulation anatoxin-a when
80 administrated by natural oral pathways, and its subsequent potential toxicological impacts on
81 organisms still exists. In a previous study, Osswald and co-workers (2007b) found that

82 anatoxin-a may be bioaccumulated by carps in significant levels ($0.768 \mu\text{g.g}^{-1}$ of carp weight).
83 Whether this may have an impact in aquatic food webs is not yet known.

84
85 In this study, we wanted to study the toxicokinetics of the anatoxin-a and its consecutive
86 possibility of accumulation in fish tissues. We use medaka model fish in order to be able to
87 administrate, under controlled conditions by a single gavage, predetermined dose of anatoxin-
88 a in order to determine the dose-response toxicity parameters and to follow the
89 assimilation/depuration processes of fish gavaged with a no observable adverse effect level
90 (NOAEL) dose during the 10 following days. As there is still a lack of reference and
91 standardized protocol for anatoxins-a extraction from biological matrix, such as fish tissues,
92 and for quantification analysis, we have also tested three different extraction procedures
93 inspired by previously published works (Triantis et al., 2016) and describe a high accuracy
94 detection method developed on UHPLC coupled HR-qTOF mass spectrometer using TASQ
95 software. This present work provides significant outcomes for the investigation of fish
96 contamination by anatoxin-a.

97
98 **Material and methods**

99 *Chemicals*

100 In solution certified (+)-Anatoxin-a and dry (\pm)-Anatoxin-a were purchased from CRM-
101 NRC (Canada) and Abcam (UK), respectively. The purity and the concentration of the daily
102 reconstituted (\pm)-Anatoxin-a in ultra-pure water was initially checked by LC-MS/MS as
103 described in the following protocol. UHPLC-MS grade methanol and acetonitrile were
104 purchased from Bio TechnoFix (France). Proteomics grade formic acid was purchased from
105 Sigma-Aldrich (Germany).

106
107 *Cyanobacteria cultures and Anatoxin-a extraction procedure test*

108 Three monoclonal non-axenic cultures of *Phomidium* sp. (PMC 1001.17, 1007.17 and
109 1008.17) maintained at 25°C in 15-mL vessels with Z8 media in the PMC (Paris Museum
110 Collection) of living cyanobacteria. Larger volume of all strains was simultaneously cultivated
111 during one month in triplicates in 250 mL Erlenmeyer vessels at 25°C using a Z8 medium with
112 a 16h:8h light/dark cycle ($60 \mu\text{mol.m}^{-2}.\text{s}^{-1}$). Cyanobacterial cells were centrifuged (at 4,000 g
113 for 10 min), then freeze-dried and stored at -80°C prior to anatoxin-a extraction. The
114 lyophilized cells were weighted, sonicated 2 min in a constant ratio of 100 μL of solvent for 1
115 mg of dried biomass, centrifuged at 4°C (12,000 g; 10 min), then the supernatant was collected
116 and directly analysed by mass spectrometry. We have presently tested in triplicates the
117 extraction efficiency of three different solvent mixtures already propositioned for anatoxin-a
118 extraction (Bogialli et al., 2006; Rellan et al., 2007; Triantis et al., 2016; Haddad et al., 2019),
119 comprising: a pure water solution acidified with 0.1% formic acid (“Water” extraction), a 25-
120 % acetonitrile solution acidified with 0.1% formic acid (“Acetonitrile” extraction), and a 75-%
121 methanol solution acidified with 0.1% formic acid (“Methanol” extraction). The efficiency of
122 the extraction procedure was significantly determined according to Dunn’s post-hoc test
123 performed after Krustal-Wallis non-parametric tests process on R software.

124
125 *Fish experimentation*

126 Experiments on medaka fish was conducted according to European community good
127 practices, validated by the ethical “comité Cuvier” (Author. APAFiS#19417-
128 2019022711043436 v4) and under the supervision of accredited personnel (B.M.). Adult female
129 medaka fishes (*Oryzias latipes*) of the inbred cab strain and of above 1 ± 0.1 g of wet weight
130 were used in all experiments. They were raised in 20-L glass aquaria filled with a continuously
131 aerated mixture of tap water and reverse osmosis filtered water (1/3–2/3, respectively), which
132 was changed once a week. Fish were maintained at 25 ± 1 °C, with a 12 h:12 h light:dark
133 standard cycle.

134 Fish were individually anesthetized in 0.1% tricaine methane sulfonate (MS-222; Sigma, St.
135 Louis, MO), and then, briefly, 2 μ L of a (\pm)-anatoxin-a mixture containing from 0.2 to 20 μ g
136 of (\pm)-anatoxin-a in water saturated with phenol red dyes was administrated by gavage
137 performed with a smooth plastic needle. Control fishes were gavaged with 2 μ L of water
138 saturated with phenol red dyes. For all individual, the efficiency of the gavage uptakes was
139 carefully checked according to the total lack of phenol red release from the mouth or the gill
140 opercula of the fish, otherwise the individual was immediately sacrificed. The fish was then
141 instantaneously placed in fresh water tanks and individually observed during 30 min in order
142 to detect any behavioural sign of anatoxin-a neurotoxicity, that comprises: paralysis, decrease
143 of breathing activity through opercular movements, locomotors activity or buoyancy default.
144 Indeed, when gavaged with none toxic dose or control mixture, fish promptly recovers from
145 anaesthesia within a minute and rapidly normal swimming activity (in less than 3-5 minutes).
146 But, alternatively, the toxicological effects of toxic doses of (\pm)-anatoxin-a induce immediate
147 neuro-muscular pathology and provoke a full breathing stop. After 30 min of observation, the
148 individual was declared as “dead” as no recover was observed and the experiment was then
149 concluded, then all fishes were anesthetized in 0.1% tricaine methane sulfonate (MS-222) and
150 euthanized. The medium lethal dose (LD_{50}) and the no observable adverse effect limit
151 (NOAEL) were calculated from toxicological results by logistic regression after log
152 transformation of the concentration values using R software.

153 For toxico-kinetics investigations, adult female medaka fish were similarly gavaged
154 individually by a single NOAEL dose, then placed in fresh water and collected after 1h, 3h, 6h,
155 12h, 24h, 3d, 7d or 10d of maintaining under classical conditions. Accordingly, all fishes were
156 anesthetized in 0.1% tricaine methane sulfonate, sacrificed, dissected, and the whole gut, the
157 liver and the muscles were sampled and flash-frozen in liquid nitrogen, and kept frozen at -
158 80°C prior to analysis.

159

160 *Anatoxin-a and metabolite extraction from fish tissues*

161 The fish tissues were weighted then sonicated 2 min in a constant ratio of 10 μ L of 75%-
162 methanol solution acidified with 0.1% formic acid for 1 mg of wet biomass for guts and livers,
163 and of lyophilised biomass for muscles, grinded into a fine powder on Tissue-lyser (with 5 mm
164 steel beads, Qiagen), centrifuged at 4°C (12,000 g; 10 min); then the supernatant was collected
165 and directly analysed by mass spectrometry. The efficiency of the extraction was estimated
166 according to the recovery rate determined in triplicats by injecting known amount of (\pm)-
167 anatoxin-a to negative samples before extraction (method A) or just before the mass
168 spectrometry analysis (method B).

169

170 *Anatoxin-a detection and quantification*

171 Ultra high performance liquid chromatography (UHPLC) was performed on 2 μ L of each of
172 the metabolite extracts using a Polar Advances II 2.5 pore C₁₈ column (Thermo) at a 300
173 μ L.min⁻¹ flow rate with a linear gradient of acetonitrile in 0.1% formic acid (5 to 90 % in 21
174 min). The metabolite contents were analyzed in triplicate for each strain using an electrospray
175 ionization hybrid quadrupole time-of-flight (ESI-QqTOF) high resolution mass spectrometer
176 (Maxis II ETD, Bruker) at 2 Hz speed on simple MS mode and subsequently on broad-band
177 Collision Ion Dissociation (bbCID) MS/MS mode on the 50–1500 m/z rang. Calibrants,
178 composed by serial dilutions of (+)-anatoxin-a, and negative control (phenylalanine) were
179 analysed similarly. The raw data were automatically process with the TASQ 1.4 software for
180 internal recalibration (< 0.5 ppm for each sample, as an internal calibrant of Na formate was
181 injected at the beginning of each analysis) for global screening and quantification, and
182 molecular featuring, respectively. Then, the automatic screening and quantification of anatoxin-
183 a was performed with threshold parameters set to recommended default value for the Maxis II
184 mass spectrometer (Δ RT < 0.4 s, Δ m/z < 3 ppm, mSigma < 50 and S/N < 5). Quantification
185 was performed according to the integration of the area under the peaks and calibration curve
186 was performed with certified standards.

187

188 *Analysis of liver metabolomes*

189 Metabolites composition of the fish livers were analysed by injection of 2 μ L of the 75%
190 methanol extracts on an UHPLC (ELUTE, Bruker) coupled with a high-resolution mass
191 spectrometer (ESI-Qq-TOF Compact, Bruker) at 2 Hz speed on simple MS mode and
192 subsequently on broad-band Collision Ion Dissociation (bbCID) or autoMS/MS mode on the
193 50–1,500 m/z rang. The analyte annotations were performed according to precise mass and
194 isotopic and fragmentation MS/MS patterns, as previously described (Kim Tiam et al., 2019).
195 The feature peak list was generated from recalibrated MS spectra (< 0.5 ppm for each sample,
196 as an internal calibrant of Na formate was injected at the beginning of each analysis) within a
197 1–15 min window of the LC gradient, with a filtering of 5,000 count of minimal intensity, a
198 minimal occurrence in at least 50% of all samples, and combining all charge states and related
199 isotopic forms using MetaboScape 4.0 software (Bruker). The intensity data table of the 591
200 extracted analytes was further treated using MetaboAnalyst 4 tool (Chong et al., 2019) for
201 Pareto's normalization, ANOVA, PCA and PLS-DA, and data representation by heatmap with
202 hierarchical clustering, loading plots and box plots.

203 Unsupervised PCA models were first used to evaluate the divide between experimental
204 groups, while supervised PLS-DA models allowed us to increase the separation between sample
205 classes and to extract information on discriminating metabolites. The PLS-DA allowed the
206 determination of discriminating metabolites using the analytes score values of the variable
207 importance on projection (VIP) indicating the respective contribution of a variable to the
208 discrimination between all of the experimental classes of samples. The higher score being in
209 agreement with a strongest discriminatory ability and thus constitutes a criterion for the
210 selection of the analytes as discriminative components. The PLS models were tested for over
211 fitting with methods of permutation tests. The descriptive, predictive and consistency
212 performance of the models was determined by R², Q² values and permutation test results (n =
213 100), respectively.

214

215 Results

216 *Anatoxin-a extraction and analysis*

217 Anatoxin-a specific mass spectrometry detection and quantification was automatically
218 determined with high accuracy using TASQ (Bruker, Germany) from raw data generated by
219 LC-MS/MS system according to the observation of analytes signal exhibiting targeted precise
220 molecular mass, retention time, isotopic pattern and fragmentation ions (Fig. 1A-B). This
221 approach allows to discriminate both (+)-anatoxin-a and (-)-anatoxin-a isomers according to
222 their respective retention times (Fig. 1C), as well as phenylalanine (Fig. 1D) used as negative
223 control, that does not exhibit any signal interaction with the anatoxin-a quantification. Standard
224 solutions containing certified quantity of (+)-anatoxin-a was diluted in ultra-pure water in the
225 range of $5 \mu\text{g.mL}^{-1}$ - 2 ng.mL^{-1} and used for calibration with good linearity of the calibration
226 curve exhibiting a correlation coefficient with $R^2 = 0.99326$ (Fig. 1E). Quantification of the
227 (+)-anatoxin-a was performed according to the area-under-the-curve signal that was
228 automatically integrated and process by the software that provide calculation details comprising
229 all diagnostic elements in the report table generate for each analysis (Fig 1F).

230 Anatoxin-a extraction efficiency was assayed in triplicates with 3 different *Phormidium*
231 strains using rather acetonitrile, methanol or water solvent solutions. In our hands, the 75%
232 methanol acidified with 0.1% formic acid present significantly higher efficiency for anatoxin-
233 a extraction (Table 1) and was further performed for the fish tissue extraction. Instrument and
234 method detection and quantitation limits (LOD and LOQ) and recovery rate were determined
235 by using triplicate injections of the control different fish tissues spiked with of determined doses
236 of (+)-anatoxin-a that were administrated before the extraction (method A), or just before the
237 sample analysis by mass spectrometry (method B) (table 2). The LOD and LOQ of the technics
238 was estimated to be in the same rang as those previously described (Triantis et al., 2016). These
239 investigations also show that anatoxin-a extraction and detection recovery rate vary from 25-
240 78% and 51-126%, respectively, according to the tissue analysis with the guts and the muscles
241 presenting the best and the worth recovery scores, respectively.

242

243 *Anatoxin-a toxicology*

244 All individuals, including negative controls, gavaged with (\pm)-anatoxin-a doses up to $6.67 \mu\text{g.g}^{-1}$
245 survive without presenting any apparent symptoms of toxicosis and were able to recover
246 from the tricaine sedation within less than 3 minutes when placed in fresh water. On contrary,
247 all individual gavaged with $20 \mu\text{g.g}^{-1}$ (\pm)-anatoxin-a rapidly present (in the first 5 minutes)
248 obvious signs of neurotoxic effects, comprising a complete stop or a rapid diminution of
249 opercular movement, abnormal swimming with hemi- or complete paresis of the fins,
250 accompanied with a global musculature rigidity. After 10 min, only one individual even
251 presents few sporadic breathing activity, that completely stop after 15 min, when all other
252 organisms already present complete paresis and ventilation cease. After 30 min, these
253 individuals, presenting no sign of recovery, were considered as dying, if not dead, and
254 euthanized, then were considered for further toxicological dose calculation. When LD₁₀₀ and
255 the NOAEL were observed at $20 \mu\text{g.g}^{-1}$ and $6.67 \mu\text{g.g}^{-1}$ (\pm)-anatoxin-a, respectively, the LD 50
256 was calculated as $11.5 \mu\text{g.g}^{-1}$ of (\pm)-anatoxin-a (Fig. 2A; table 3).

257

258 *Anatoxin-a toxicokinetics*

259 Following gavage experiment of adult female medaka fish to NOAEL, we have quantified
260 (\pm)-anatoxin-a in the guts, the livers and the muscles after 1h, 3h, 6h, 12h, 24h, 3d, 6d and 10d,
261 in order to monitor the dynamic of the anatoxin-a assimilation/depuration efficiency in these
262 various compartments (Fig. 1B-D). The highest (\pm)-anatoxin-a amount was observed just 1h
263 after the exposure, representing up to $15,789 \mu\text{g.g}^{-1}$ in some individual livers, representing more
264 than 100 times more anatoxin-a than in the livers of other organisms similarly gavaged,
265 illustrating the relative individual variability of the anatoxin-a uptake and
266 assimilation/elimination during our experimentation. Although, fish tissues present a global
267 individual variability, the larger amount of anatoxin-a were observed in livers, the guts, and in
268 a lesser amount in the muscles after 1h, then the tissues present a rapidly decrease of anatoxin-
269 a contents. Almost no more anatoxin-a was detectable after 24h in all tissues. The depuration
270 rate was calculated for the 12 first hours of depuration as being of 57, 100 and 90%, in guts,
271 livers and muscles, respectively, leading to a rapid elimination of the anatoxin-a that does no
272 seems to bio-accumulate in any of the investigated fish tissues.

273

274 *Anatoxin-a effects on the liver metabolome*

275 In order to investigate the molecular effects induced by (\pm)-anatoxin-a NOAEL exposure,
276 the liver metabolite composition was compared between ungavaged fish (control) and fish
277 collected 1h, 3h, 6h, 12h or 24h after gavage. The same livers extracts than those extracted with
278 75% methanol and analysed for anatoxin-a quantification were investigated by LC-MS/MS for
279 untargeted metabolomics. A total of 591 different analytes were then extracted by the optimized
280 pipeline, and their respective quantification (determined from the area-under-the-peak signal)
281 compared between the different time-course groups using multivariate statistical methods,
282 including unsupervised principal component analysis (PCA) and supervised partial least-
283 squares discriminate analysis (PLS-DA), together with univariate groups variance analyses
284 (ANOVA), in order to evaluate the potential of the method to discriminate among the
285 experimental groups according to the time-course of anatoxin-a exposure and elimination.

286 Although the analysed fish livers present a global metabolome variability (Fig. 3A), the (\pm)-
287 anatoxin-a gavage seems to rapidly modify the specific amount of various metabolites which
288 progressively retrieved their initial state, as observed on components 1-3 projection of the PCA
289 (Fig. 3B). The 29 analytes that present significant variation between the different groups
290 according to ANOVA ($P < 0.05$) indicate a clear difference between the groups, as observed on
291 heatmap with hierarchical clustering (Fig. 3D), with a rapid increase or decrease of the
292 metabolite quantity that diminishes after few hour and almost recover control levels after 24h
293 post-gavage (Fig. 3E). The supervised multivariate analysis (PLS-DA) model shows consistent
294 R^2 cumulative, Q^2 cumulative and permutation scores (Fig. 3F). The most discriminating m/z
295 features in the PLS-DA model (Figure 3C) were selected based on their respective VIP score,
296 which resulted in 25 compounds with VIP value higher than 2 (Table 4), on component 1 and/or
297 2 (both contributing to the experimental group discrimination). The molecular formulas of each
298 VIP were proposed based on accurate mass measurement, true isotopic pattern, and their
299 putative identification were attempted with Metfrag and GNPS according to additional
300 respective MS/MS fragmentation patterns. Interestingly, the tricaine (MW 165.0794 Da)

301 belong to this VIP list and presents, as one could expect, a clear increase between the Control
302 and 1h post-gavage fish livers (in relation with pre-gavage anesthesia procedure by balneation
303 in 0.1% tricaine), then a complete disappearance between 1 and 3h.

304 The list of other putatively annotated compounds comprises then various phospholipids
305 (n=9) belonging to the glycerol-phosphocholine group, all presenting comparable variation
306 patterns among the experimental groups, with an initial drop of these metabolite quantity
307 between the control and the 1h group, then a progressive re-increase until an almost complete
308 recovery of the initial metabolite amount within less than 24h. Those metabolites are directly
309 related to lipid metabolism process and their successive decrease and increase within the liver
310 may denote an important lipid consumption by the organism and a progressive recover of the
311 liver to an unstressed condition. On the contrary, the sole VIPs which relative quantities present
312 an initial increase were an undetermined analyte (MW 1064.600 Da) and the adenosine, both
313 retrieving their initial levels within less than 24h. Such adenosine transient increase may denote
314 an intensification of hepatic blood circulation, as it presents direct effect on vasodilation of liver
315 arteria (Robson & Schuppan 2010). Although our experimental design does allow to
316 discriminate the specific effects of the anatoxin-a from those of the tricaine anesthesia alone, it
317 overall shows that the organisms present a complete recovery 24h after being gavaged with
318 anatoxin-a single NOAEL dose.

319

320 Discussion

321 In the present study, the neurotoxicological response of medaka fish subjected to anatoxin-a
322 appears comparable to that found in carp (Osswald et al., 2007a) and zebrafish (Carneiro et
323 al., 2015) supporting the evidences for the existence of a similar mechanism of action. Whereas
324 no apparent precursor effect appears when fish are gavaged with sub-acute doses of anatoxin-a,
325 the symptoms observed in the fish exposed to a higher dose denote an all-or-nothing effect,
326 comprising rapid and intense neurotoxic signs, that are compatible with the mechanism of toxic
327 action of anatoxin-a in the nervous system that has been described so far for other vertebrates
328 (Fawell et al., 1999). These symptoms comprise different manifestations of muscular paralysis
329 that are likely due to the primary, and nearly irreversible, binding of the anatoxin-a, being an
330 acetylcholine antagonist, to the acetylcholine receptors of the cholinergic synapses of the
331 neuromuscular junctions, leading to a continuous muscular contraction. Previous works
332 indicate that below a certain levels the effects appear to be transient, the animals being able to
333 make a complete and rapid recovery, although the data available in the literature remains limited
334 (Dittman and Wiegand 2006).

335 Our dose-response toxicological analysis indicates that anatoxin-a exhibits toxicological
336 reference dose of 5.75 and 3.33 $\mu\text{g.g}^{-1}$ of medaka body weight for LD₅₀ and NOAEL,
337 respectively. This results are in remarkable agreement with precedent data obtained on other
338 organisms. Indeed, previous investigations of anatoxin-a toxicity determined on mouse that,
339 when administrated by single dose gavage, (+)-anatoxin-a exhibits a LD₅₀ and a NOAEL of
340 above 5 and 3 $\mu\text{g.g}^{-1}$ of body weight, respectively (Fawell et al., 1999). In addition, Stevens and
341 co-workers (1991) have initially shown that (+)-anatoxin-a presents LD₅₀ value of 16.2 and 6.7
342 $\mu\text{g.g}^{-1}$ of body weight, for pure (+)-anatoxin-a and complex extract containing anatoxin-a
343 administrated by single gavage to mouse. Taken together, those results suggest that medaka
344 fish and mouse apparently present very similar toxicological dose-response to anatoxin-a.

345 Indeed, as the unnatural (-)-anatoxin-a isomer was shown to insignificantly contribute to the
346 global toxicity to the 1/1 racemic mixture of (\pm)-anatoxin-a used in this study (MacPhail et al.,
347 2007), one could estimate that toxicity values of (+)-anatoxin-a might theoretically be very
348 similar for medaka fish than for mouse.

349
350 In our experiments, the promptitude of the neuromuscular effects of anatoxin-a when
351 administrated by gavage are in agreement with previous investigation performed on mice
352 (Fawell et al., 1999), suggesting that anatoxin-a might be rapidly assimilated by the organisms
353 by crossing the intestine barrier and being widespread to the whole musculature within less than
354 2 minutes. When anatoxin-a producing cyanobacterial biofilm are accidentally ingested by dogs,
355 the animals present first appearance of neurotoxic symptoms within less than 5 minutes (Wood
356 et al., 2007), testifying for a very rapid assimilation of a toxinogenous dose of anatoxin-a
357 released from the cyanobacterial biomass within the stomach. To date, the genuine mechanism
358 of the anatoxin-a transfer through the intestinal epithelia remains undetermined but the
359 promptitude of the effects suggests that this small molecule (MW = 165 da) may remain
360 uncharged in order to be able to sharply cross the intestinal barrier, potentially through passive
361 paracellular diffusion (Dahlgren and Lennernäs 2019).

362 Our toxico-kinetics investigation has shown that no detectable amount of anatoxin-a was
363 still observed in guts 12h after the fish having been gavaged to a single NOAEL dose. Then,
364 the medaka fish presents also a rapid elimination of the anatoxin-a that transiently have been
365 addressed to the liver, and in a lesser extent to the muscle, indicating that it may not be
366 apparently accumulating anatoxin-a under those conditions. Interestingly, Osswald and co-
367 workers (2011) have shown no significant bioaccumulation of anatoxin-a in the trout tissues
368 when administrated by balneation up to 5 mg.L⁻¹ of anatoxin-a. Previously, Osswald et al.
369 (2008) have also similarly shown no bioaccumulation of anatoxin-a by the Mediterranean
370 mussel *M. galloprovincialis*, that has been otherwise shown to present high accumulation
371 capability for various contaminants, such as microcystins (Vasconcelos 1995). Although they
372 observed some anatoxin-a uptake from the surrounding water filtered by the animals (observed
373 maximum accumulation efficiency = 11%), this seemed rapidly reduced rather by the
374 depuration process of phase II detoxification enzymes or by passive elimination processes.
375 These data show that, as anatoxin-a is capable to rapidly penetrate the whole organisms body,
376 and induces obvious and acute neurotoxicological effects within a minute, it may also be rapidly
377 eliminated by classical excretion or depuration mechanisms.

378

379 Conclusion

380 In our gavage experiment of medaka fish to a single NOAEL dose of anatoxin-a, the toxin
381 appears to have been rapidly eliminated and the molecular effects were no more perceptible
382 within the fish liver metabolome after 24h.

383 These observations suggest that when the dose remains below the acute toxicological limit
384 producing neurotoxicosis that can lethal consequences, the organism are able to make a
385 completely and rapidly recovery, that seems not to induce obvious effects even if the exposure
386 is repeated several times (Fawell et al. 1999). However, one could still suspect that chronic
387 anatoxin-a exposure may induce more insidious long-term pathologies on the central nervous
388 system (Lombardo and Maskos 2015). But this hypothesis still remains to be explored.

389 More over, the accurate investigations of the fish flesh contamination by anatoxin-a under
390 highest toxinogenous cyanobacterial proliferations, especially when, in nature, certain fish are
391 potentially actively feeding on those biofilms (Ledreux et al., 2014), still remain to be
392 performed in order to provide convincing data supporting the evaluation of the associated risks.
393
394

395 **Acknowledgements**

396 This work was supported by grant CRD from ANSES attributed to the Cyanariv project, lead
397 by Catherine Quiblier.
398

399 *The authors declare not conflict of interest*
400
401

402 **References**

403 Aboal, M., Puig, M. A., Mateo, P., & Perona, E. (2002). Implications of cyanophyte toxicity on biological
404 monitoring of calcareous streams in north-east Spain. *Journal of Applied Phycology* 14(1), 49-56.
405 Anderson, B., Voorhees, J., Phillips, B., Fadness, R., Stancheva, R., Nichols, J., ... & Wood, S. A. (2018).
406 Extracts from benthic anatoxin-producing *Phormidium* are toxic to 3 macroinvertebrate taxa at
407 environmentally relevant concentrations. *Environmental toxicology and chemistry* 37(11), 2851-2859.
408 Aráoz, R., Molgó, J., & De Marsac, N. T. (2010) Neurotoxic cyanobacterial toxins. *Toxicon* 56(5), 813-828.
409 Bogialli, S., Bruno, M., Curini, R., Di Corcia, A., & Laganà, A. (2006). Simple and rapid determination of
410 anatoxin-a in lake water and fish muscle tissue by liquid-chromatography–tandem mass spectrometry.
411 *Journal of Chromatography A* 1122(1-2), 180-185.
412 Bouma-Gregson, K., Kudela, R. M., & Power, M. E. (2018). Widespread anatoxin-a detection in benthic
413 cyanobacterial mats throughout a river network. *PloS One* 13(5), e0197669.
414 Carmichael, W. W., Biggs, D. F., & Gorham, P. R. (1975). Toxicology and pharmacological action of
415 *Anabaena flos-aquae* toxin. *Science* 187(4176), 542-544.
416 Carmichael, W. W. (1994). The toxins of cyanobacteria. *Scientific American* 270(1), 78-86.
417 Carneiro, M., Gutierrez-Praena, D., Osorio, H., Vasconcelos, V., Carvalho, A. P., & Campos, A. (2015).
418 Proteomic analysis of anatoxin-a acute toxicity in zebrafish reveals gender specific responses and
419 additional mechanisms of cell stress. *Ecotoxicology and environmental safety* 120, 93-101.
420 Chong, J., Wishart, D. S., & Xia, J. (2019). Using metaboanalyst 4.0 for comprehensive and integrative
421 metabolomics data analysis. *Current protocols in bioinformatics* 68(1).
422 Dahlgren, D., & Lennernäs, H. (2019). Intestinal Permeability and Drug Absorption: Predictive
423 Experimental, Computational and *In Vivo* Approaches. *Pharmaceutics* 11(8), 411.
424 Dittmann, E., & Wiegand, C. (2006). Cyanobacterial toxins—occurrence, biosynthesis and impact on human
425 affairs. *Molecular nutrition & food research* 50(1), 7-17.
426 Fawell, J. K., Mitchell, R. E., Hill, R. E., & Everett, D. J. (1999). The toxicity of cyanobacterial toxins in the
427 mouse: II anatoxin-a. *Human & experimental toxicology* 18(3), 168-173.
428 Gugger, M., Lenoir, S., Berger, C., Ledreux, A., Druart, J. C., Humbert, J. F., ... & Bernard, C. (2005). First
429 report in a river in France of the benthic cyanobacterium *Phormidium favosum* producing anatoxin-a
430 associated with dog neurotoxicosis. *Toxicon* 45(7), 919-928.
431 Greer, B., Maul, R., Campbell, K., & Elliott, C. T. (2017) Detection of freshwater cyanotoxins and
432 measurement of masked microcystins in tilapia from Southeast Asian aquaculture farms. *Analytical and*
433 *Bioanalytical Chemistry* 409(16), 4057-4069.
434 Haddad, S. P., Bobbitt, J. M., Taylor, R. B., Lovin, L. M., Conkle, J. L., Chambliss, C. K., & Brooks, B. W.
435 (2019). Determination of microcystins, nodularin, anatoxin-a, cylindrospermopsin, and saxitoxin in water

436 and fish tissue using isotope dilution liquid chromatography tandem mass spectrometry. *Journal of*
437 *chromatography. A* 1599, 66.

438 Kim Tiam, S., Gugger, M., Demay, J., Le Manach, S., Duval, C., Bernard, C., & Marie, B. (2019). Insights
439 into the Diversity of Secondary Metabolites of *Planktothrix* Using a Biphasic Approach Combining
440 Global Genomics and Metabolomics. *Toxins* 11(9), 498.

441 Ledreux, A., Brand, H., Chinain, M., Bottein, M. Y. D., & Ramsdell, J. S. (2014). Dynamics of ciguatoxins
442 from Gambierdiscus polynesiensis in the benthic herbivore Mugil cephalus: trophic transfer implications.
443 *Harmful Algae* 39, 165-174.

444 Lombardo, S., & Maskos, U. (2015). Role of the nicotinic acetylcholine receptor in Alzheimer's disease
445 pathology and treatment. *Neuropharmacology* 96, 255-262.

446 MacPhail, R. C., Farmer, J. D., & Jarema, K. A. (2007). Effects of acute and weekly episodic exposures to
447 anatoxin-a on the motor activity of rats: comparison with nicotine. *Toxicology* 234(1-2), 83-89.

448 Oberemm, A., Becker, J., Codd, G. A., & Steinberg, C. (1999). Effects of cyanobacterial toxins and aqueous
449 crude extracts of cyanobacteria on the development of fish and amphibians. *Environmental Toxicology: An International Journal* 14(1), 77-88.

450 Osswald, J., Rellan, S., Gago, A., & Vasconcelos, V. (2007a). Toxicology and detection methods of the
451 alkaloid neurotoxin produced by cyanobacteria, anatoxin-a. *Environment international* 33(8), 1070-1089.

452 Osswald, J., Rellán, S., Carvalho, A. P., Gago, A., & Vasconcelos, V. (2007b). Acute effects of an anatoxin-
453 a producing cyanobacterium on juvenile fish—Cyprinus carpio L. *Toxicon* 49(5), 693-698.

454 Osswald, J., Rellán, S., Gago, A., & Vasconcelos, V. (2008). Uptake and depuration of anatoxin-a by the
455 mussel *Mytilus galloprovincialis* (Lamarck, 1819) under laboratory conditions. *Chemosphere* 72(9),
456 1235-1241.

457 Osswald, J., Azevedo, J., Vasconcelos, V., & Guilhermino, L. (2011). Experimental determination of the
458 bioconcentration factors for anatoxin-a in juvenile rainbow trout (*Oncorhynchus mykiss*). *Proceedings of the International Academy of Ecology and Environmental Sciences* 1(2), 77.

459 Puschner, B., Pratt, C., & Tor, E. R. (2010). Treatment and diagnosis of a dog with fulminant neurological
460 deterioration due to anatoxin-a intoxication. *Journal of veterinary emergency and critical care* 20(5), 518-
461 522.

462 Quiblier, C., Wood, S. A., Echenique-Subiabre, I., Heath, M., Villeneuve, A., & Humbert, J. F. (2013). A
463 review of current knowledge on toxic benthic freshwater cyanobacteria—ecology, toxin production and
464 risk management. *Water Research* 47(15), 5464-5479.

465 Rellán, S., Osswald, J., Vasconcelos, V., & Gago-Martinez, A. (2007). Analysis of anatoxin-a in biological
466 samples using liquid chromatography with fluorescence detection after solid phase extraction and solid
467 phase microextraction. *Journal of Chromatography A* 1156(1-2), 134-140.

468 Robson, S. C., & Schuppan, D. (2010). Adenosine: tipping the balance towards hepatic steatosis and fibrosis.
469 *Journal of hepatology* 52(6), 941-943.

470 Sivonen, K., Jones, G. (1999) Cyanobacterial toxins. In: Chorus, I., Bartram, J. (Eds.), *Toxic Cyanobacteria in Water: a Guide to Their Public Health Consequences, Monitoring and Management*. E & FN Spon,
471 London, pp. 41–111.

472 Stevens, D. K., & Krieger, R. I. (1991). Stability studies on the cyanobacterial nicotinic alkaloid satoxin-A.
473 *Toxicon* 29(2), 167-179.

474 Triantis, T. M., Kaloudis, T., & Hiskia, A. (2016). Determination of Anatoxin-a in Filtered and Drinking
475 Water by LC-MS/MS. *Handbook of Cyanobacterial Monitoring and Cyanotoxin Analysis*, 408-412.

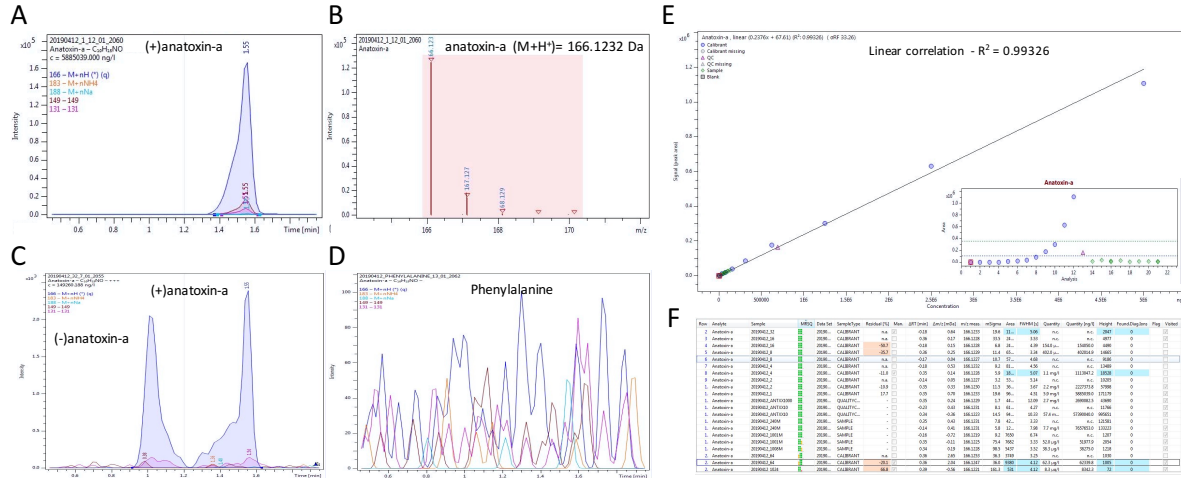
476 Vasconcelos, V. M. (1995). Uptake and depuration of the heptapeptide toxin microcystin-LR in *Mytilus galloprovincialis*. *Aquatic Toxicology* 32(2-3), 227-237.

477 Wonnacott, S., & Gallagher, T. (2006). The chemistry and pharmacology of anatoxin-a and related
478 homotropanes with respect to nicotinic acetylcholine receptors. *Marine Drugs* 4(3), 228-254.

479 Wood, S. A., Selwood, A. I., Rueckert, A., Holland, P. T., Milne, J. R., Smith, K. F., ... & Cary, C. S. (2007).
480 First report of homoanatoxin-a and associated dog neurotoxicosis in New Zealand. *Toxicon* 50(2), 292-
481 301.

486 Figure 1.

487

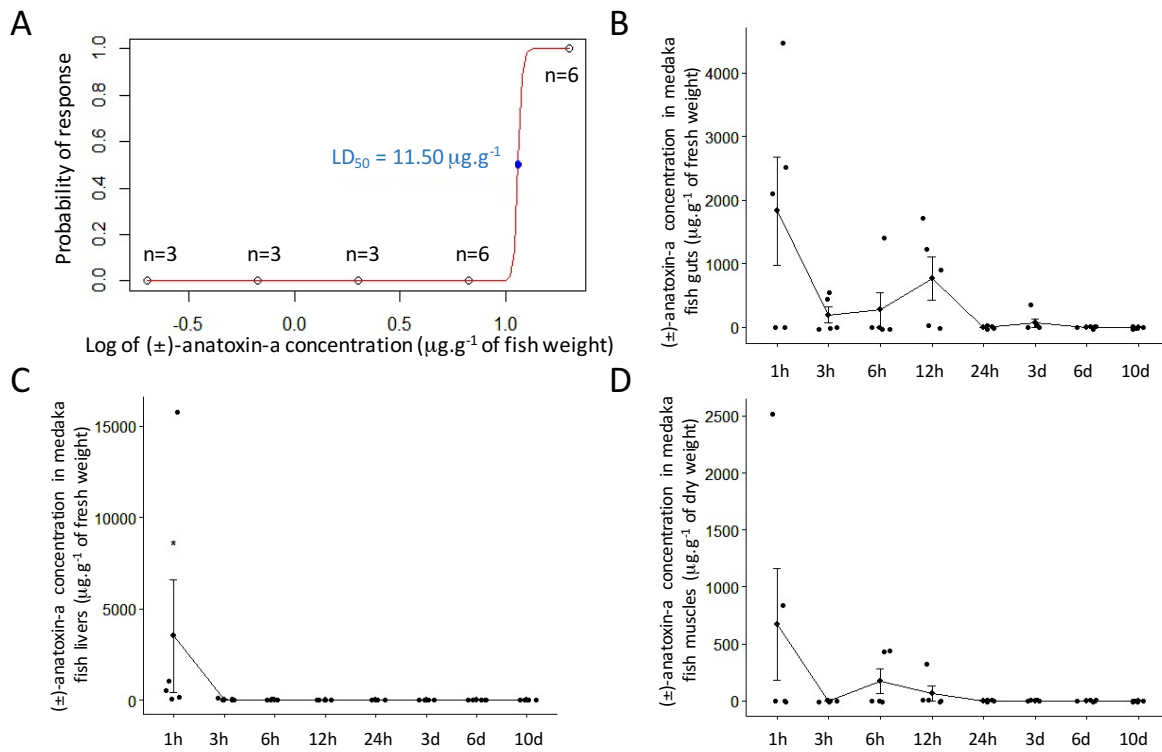


488 Figure 1. Anatoxin-a detection and quantification on HR qTOF mass spectrometer coupled to an UHPLC.
489 The screening of (+)-anatoxin-a was performed according to the specific detection of analytes presenting
490 accurate mass of the parent ion ($M+H^+ = 166.1232 \pm 0.001$ Da), accurate retention time (1.55 ± 0.2 min),
491 accurate isotopic pattern ($mSigma < 50$) and co-detection of characteristic fragment ions (149.096 ± 0.001
492 and 131.086 ± 0.001 Da) (A-B). The similar analyses of the (±)-anatoxin-a can discriminate the (-) and the
493 (+)-anatoxin-a that exhibits distinct retention times (1.1 and 1.6 min, respectively) (C). No signal was
494 detected with phenylalanine (D). Calibration curve performed with 12 serial dilutions of certified standard
495 of (+)-anatoxin-a (NRC, Canada) presenting applicable correlation factor (E). Example of screening
496 diagnostic table provided by TASQ® software for (+)-anatoxin-a quantification summarizing all qualitative
497 and quantitative parameters for each sample (F).

498

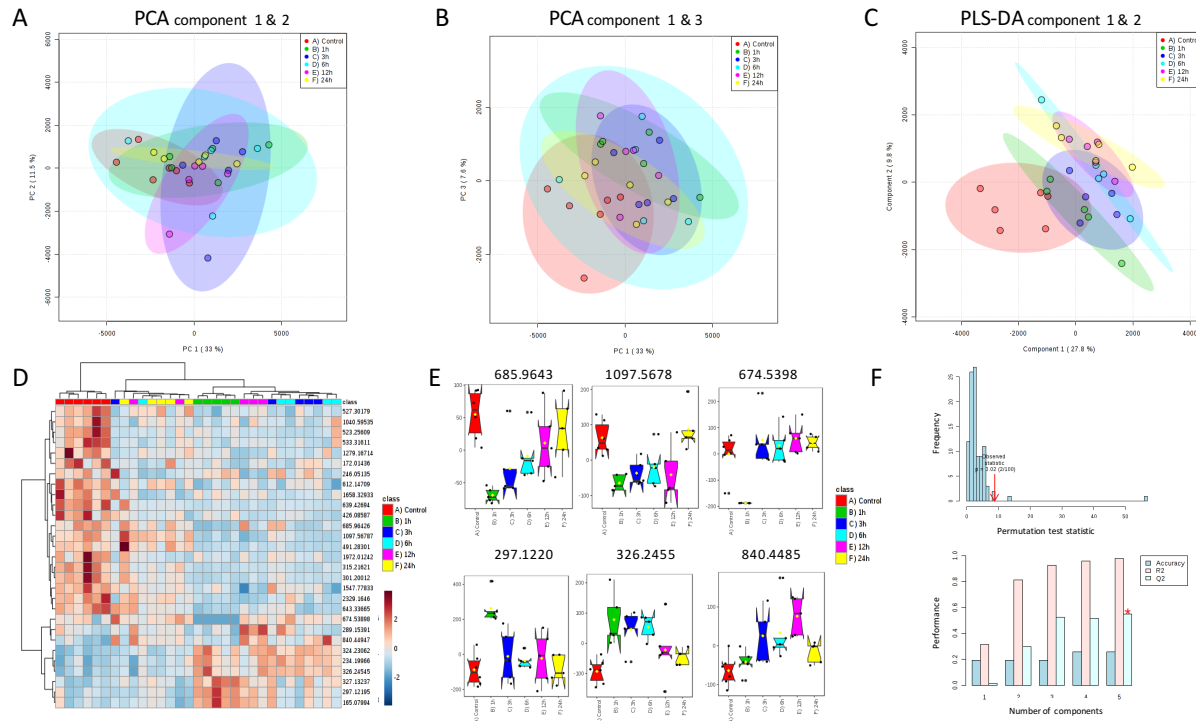
499

500 Figure 2.



501
502 Figure 2. Anatoxin-a toxicity and toxicokinetics on adult female medaka fish when administrated by single-
503 dose gavage. Estimation of the LD_{50} of (±)-anatoxin-a by linear regression after log transformation (μg of
504 (±)-anatoxin-a. g^{-1} of fish mass) (A). Toxicokinetics of (±)-anatoxin-a administrated in a single NOAEL dose
505 ($6.67 \mu\text{g.g}^{-1}$ fish weight) in the gut (B), the liver (C) and the muscle (D) after 1h, 3h, 6h, 12h, 24h, 3d, 6j or
506 10j of depuration (n=5). On the 30 investigated individuals, only 6 of them does not present detectable amount
507 of anatoxin-a, overall testifying for the global efficiency of the gavage experiments.

508 Figure 3.



509
510 Figure 3. Metabolomics investigation of the liver metabolite variations after the administrated of a single
511 NOAEL dose of (\pm)-anatoxin-a ($6.67 \mu\text{g.g}^{-1}$ fish weight) by gavage of adult female medaka fish in the liver
512 after 1h, 3h, 6h, 12h and 24h. Individual score plots generated from a principal component analysis performed
513 with the intensity count of 591 variables according to components 1-2 (A) and 1-3 (B). Heatmap
514 representation with hierarchical classification (Ward clustering according to Euclidian distances) performed
515 from relative intensities of the 29 significantly dysregulated analytes ($P < 0.05$ ANOVA) (D) and 6 examples
516 of representative box-plots (E). Individual score plot generated from PLS-DA analysis performed with 591
517 extracted variables according to components 1-2 (C), and quality descriptors of the statistical significance
518 and predictive ability of the discriminant model according to corresponding permutation and cross-validation
519 tests (F), respectively.

520

521 **Tables**

522

<i>Phormidium</i> strain	Extraction solvent		
	Acetone	Water	Methanol
PMC 1001.17	6436 ± 139 ^a	5864 ± 85 ^b	6689 ± 158 ^a
PMC 1007.17	2949 ± 148 ^b	1467 ± 88 ^c	3655 ± 147 ^a
PMC 1008.17	1773 ± 95	1420 ± 103	1913 ± 192

523

524 Table 1. Efficiency of different protocols for anatoxin-a extraction from different cyanobacterial strains. ^{a-b}-
525 ^c: indicate group results in a decreasing order of Dunn's post-hoc test performed after Krustal-Wallis non-
526 parametric tests.

527

528

Organ	Recovery rate		Limit of detection (LOD)		Limit of quantification (LOQ)	
	Method A	Method B	µg.L ⁻¹	µg.g ⁻¹	µg.L ⁻¹	µg.g ⁻¹
Intestin ^a	78 ± 13 %	126 ± 22%	0.412	20.6	1.25	62.5
Liver ^a	65 ± 7 %	86 ± 15%	0.506	2.53	1.25	62.5
Muscle ^b	25 ± 4 %	51 ± 3%	0.546	14.52	1.25	285

529

530 Table 2. Recovery rate, limit of detection (LOD), and limit of quantification (LOQ) of the two tested
531 extraction procedure (A and B, corresponding to pre-extraction or pre-analysis doping, respectively)
532 measured on intestine, liver and muscle of the medaka fish. ^a: determined on fresh weight; ^b: determined on
533 dry weight.

534

Model organism	Toxicological parameter	Toxicological values (µg.g ⁻¹)	Formulation of the toxicant	Reference
Medaka fish	LD ₅₀ by gavage	11.5	(±)-anatoxin-a	This study
Medaka fish	LD ₅₀ by gavage	5.75*	(+)-anatoxin-a	This study
Medaka fish	LD ₁₀₀ by gavage	20	(±)-anatoxin-a	This study
Medaka fish	LD ₁₀₀ by gavage	10*	(+)-anatoxin-a	This study
Medaka fish	NOAEL by gavage	6.67	(±)-anatoxin-a	This study
Medaka fish	NOAEL by gavage	3.33*	(+)-anatoxin-a	This study
Zebrafish	LD ₁₀₀ by i.p.	0.8	(±)-anatoxin-a	Carneiro et al., 2015
Mouse	LD ₅₀ by i.v.	0.1	(+)-anatoxin-a	Fawell et al., 1999
Mouse	LD ₅₀ by gavage	[1-10]	(+)-anatoxin-a	Fawell et al., 1999
Mouse	NOAEL by gavage	3	(+)-anatoxin-a	Fawell et al., 1999
Mouse	LD ₅₀ by gavage	6.7	<i>A. flos aquae</i> NRC 44-1	Stevens et al., 1991
Mouse	LD ₅₀ by gavage	16.2	(+)-anatoxin-a	Stevens et al., 1991

535

536 * determined according to the theoretical 1/1 (±)-racemic ratio, experimentally confirmed by LC-MS,
537 considering as negligible the toxicity of (-)-anatoxin-a comparing to the 150-times higher toxicity of (+)-
538 anatoxin-a (Osswald et al., 2007).

539

540

Table 3. Summary of lethal concentration estimators determined for anatoxin-a by different administration pathways on different vertebrate models.

MW(Da)	RT (min)	m/z	Annotation	Formula (neutral)	VIP Com. 1	VIP Com. 2	Pattern (C-1-3-6-12-24h)
541.3166	11.8	542.3224	1-icosapentaenoyl-sn-glycero-3-phosphocholine	C ₂₈ H ₄₈ NO ₇ P	8.40	6.37	\---
569.3474	12.8	570.3537	lysophosphatidylcholine 22:5	C ₃₀ H ₅₂ NO ₇ P	7.14	5.92	\---
525.2854	12.2	526.2908	lysophosphatidylethanolamine 22:6	C ₂₇ H ₄₄ NO ₇ P	6.62	7.32	\---
499.2704	12.7	500.3048	tauoursodeoxycholic acid	C ₂₆ H ₄₅ NO ₆ S	4.52	3.88	\ \---
519.3319	12.6	520.3384	1-linoleoyl-sn-glycero-3-phosphocholine	C ₂₆ H ₅₀ NO ₇ P	4.12	3.39	\---
1248.619	5.5	625.3167	-	C ₃₀ H ₈₈ N ₂₄ O ₂₉	3.20	2.32	\---
1134.671	12.4	1135.6760	-	C ₅₈ H ₉₀ N ₁₀ O ₁₃	3.18	3.06	\---
1248.117	5.5	625.0657	-	C ₇₀ H ₁₃₇ N ₁₇ O ₂	2.85	2.03	\ \//
1082.640	11.8	1083.6469	-	C ₅₈ H ₉₀ N ₄ O ₁₅	2.80	2.03	\---
267.0969	1.6	268.1040	adenosine	C ₁₀ H ₁₃ N ₅ O ₄	2.74	1.89	//\ \
131.0939	1.6	132.1010	leucine	C ₆ H ₁₃ NO ₂	2.66	1.92	\---
612.1471	1.6	307.0808	-	C ₂₄ H ₃₇ O ₁₂ PS ₂	2.59	1.72	\---
307.0837	1.3	308.0908	glutathione	C ₁₀ H ₁₇ N ₃ O ₆ S	2.51	2.13	\ \//
467.3016	12.0	468.3088	1-myristoyl-sn-glycero-3-phosphocholine	C ₂₂ H ₄₆ NO ₇ P	2.46	3.88	\ \ -
639.4269	4.6	320.7208	-	C ₃₁ H ₅₇ N ₇ O ₇	2.45	1.61	\---
523.2561	9.3	524.2634	-	C ₂₃ H ₄₂ NO ₁₀ P	2.44	1.55	\---
204.0911	3.5	205.0984	tryptophan	C ₁₁ H ₁₂ N ₂ O ₂	2.41	1.68	\---
165.0794	6.4	166.0868	tricaine	C ₉ H ₁₁ NO ₂	2.40	3.56	\ \---
547.3283	13.6	548.3355	-	C ₂₆ H ₃₇ N ₁₃ O	2.16	1.45	\---
1064.600	6.1	533.3073	-	C ₃₀ H ₈₄ N ₁₈ O ₂₃	1.99	2.15	//\ \
543.3335	12.7	544.3400	1-arachidonoyl-sn-glycero-3-phosphocholine	C ₂₈ H ₅₀ NO ₇ P	1.91	2.66	\ \//
1050.577	12.2	1051.5843	-	C ₅₆ H ₈₂ N ₄ O ₁₅	1.88	2.00	\---
515.3015	11.3	516.3085	lysophosphatidylcholine 18:4	C ₂₆ H ₄₆ NO ₇ P	1.87	3.46	\---
521.3476	13.6	522.3531	1-elaidoyl-sn-glycero-3-phosphocholine	C ₂₆ H ₅₂ NO ₇ P	1.80	7.50	\ \//
517.3184	11.9	518.3246	1-alpha-linolenoyl-sn-glycero-3-phosphocholine	C ₂₆ H ₄₈ NO ₇ P	1.58	2.18	\ \//

Table 4. List of the 25 VIP analytes that present score > 2 on either component 1 or component 2 of the PLS-DA analysis performed with all treatment groups, and their putative annotation according to their respective high resolution mass, isotopic and MS/MS fragmentation patterns, searched against ChEBI, PubChem, HMDB and GNPS databases. “\”, “/” and “-“ indicate when the metabolites globally decreases, increases or maintains their relative quantity between the time series, respectively.